Dissipating Oscillation Energy Through Damping Amplitude/Frequency Motion: An Oscillation Suppression Method Under Energy Perspective for Converter-Interfaced Power Systems

Zhijian Cheng
Huazhong University of Science and Technology
School of Electrical and Electronic Engineering
Wuhan, China
ZhijianChengHUST@gmail.com

Sicheng Wang*
Huazhong University of Science and Technology
State Key Laboratory of Advanced Electromagnetic Technology
Wuhan, China
sicheng_wang@hust.edu.cn

Xiaoming Yuan
Huazhong University of Science and Technology
State Key Laboratory of Advanced Electromagnetic Technology
Wuhan, China
yuanxm@mail.hust.edu.cn

***Abstract*—The penetration of power electronic converter units continues to increase, while the dynamic behavior of power systems has become increasingly intricate, giving rise to emerging electromagnetic oscillations that pose a critical threat to system stability. Conventional damping control methods not only fail to associate oscillations with the energy exchange process between grid-connected converter units and the network, but also overlook the evolutionary mechanism of AC electrical variables during oscillations. As a result, these methods are unable to dissipate oscillatory energy effectively and are often tailored to specific operating conditions. To overcome these limitations, this paper proposes a damping control method grounded in the energy exchange mechanism of converter-interfaced power systems and the physical interpretation of damping. Results verify that the amplitude/frequency-state-based method can effectively suppress emerging electromagnetic oscillations and improve system stability.**

***Index Terms*-- Amplitude/Frequency State; Damping Control; Oscillation Suppression; Power Electronic Converter Unit; System Oscillation**

I. Introduction

Driven by the continuous growth of electricity demand from economic and social development, coupled with the deepening of low-carbon philosophy, power electronic converter units have been widely deployed, fundamentally reshaping the structural and operational characteristics of power systems. The widespread deployment of power electronics converter units has rendered system dynamics increasingly intricate, resulting in emerging electromagnetic oscillations that occur more frequently and cannot be effectively mitigated by conventional methods. As a result, emerging electromagnetic oscillations have posed significant challenges to the stable and secure operation of today's power systems.

Currently, most research on oscillation suppression methods in today's power systems has focused on superficial oscillation phenomena. For the sub-synchronous oscillation problem in Hami, Xinjiang, [1] proposed an oscillation suppression method in which the oscillatory components are extracted and then processed by phase-shifting and gain control to form an additional damping control signal. Due to the occurrence of sub-synchronous interactions (SSI) phenomena in the ERCOT region, [2] designed an additional damping control for doubly-fed induction generator (DFIG) wind turbines based on a multi-input multi-output (MIMO) state-space methodology to address the problem. In addition, virtual impedance control is another widely used method for oscillations mitigation, in which the equivalent resistance around the resonance frequency is enhanced by introducing control for specific harmonics [3]-[5]. However, without considering that oscillations describe the evolution of AC electrical variables during the energy exchange between power converter units and networks, which originates from the amplitude and frequency modulation of rotating vector around corresponding operating points [6], and without reflecting that oscillatory energy drives the motion of internal-voltage amplitude/frequency, these methods fail to achieve effective dissipation of oscillatory energy and are often applicable only to specific scenarios or oscillation modes, which is reflects in the virtual impedance's parament effectiveness issues.

In view of this, guided by the requirements for the stable and safe operation of today's power systems, this research proposes a damping control method based on state variables of power electronics converter units, which is developed from operation mechanisms of converter-interfaced power systems

This work was supported in part by the National Natural Science Foundation of China under Grant U23B6008 and the Delta Power Electronics Science and Education Development Program of Delta Group under Grant DREN2023001.

* Corresponding author: Sicheng Wang

979-8-3315-8138-1

and the physical interpretation of damping. The paper proceeds as follows. Section II introduces the structure and operational mechanism of converter-interfaced power systems. Section III elucidates the energy exchange mechanism between units and networks during system dynamics, revealing that the internal-voltage frequency and amplitude serve as the grid-connected converter unit's state variables representing the grid-connected converter unit's energy level. On this basis, the amplitude/frequency state-based damping control method is proposed. Section IV validates the proposed method's effectiveness under different scenarios. Finally, Section V draws some conclusions.

II. Structure and Operating Principle of Converter-Interfaced Power Systems

A. Structure of Conerter-Interfaced Power Systems

The typical circuit and control structure of grid-interfaced units are shown in Fig. 1. The part highlighted by the green dashed box illustrates the typical structure of the current control considered in the research.

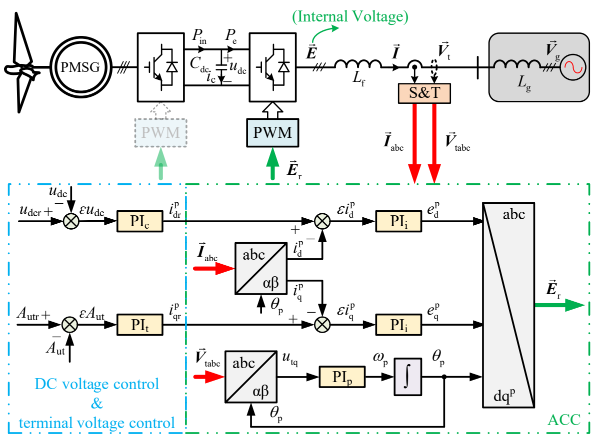

Fig. 1 Schematic diagram of the circuit and control structure of typical grid-connected converter units

The line current $\vec{I}$ flowing through the filter inductor and the voltage $\vec{V}_t$ at the point of common coupling (PCC) are measured and fed to the ACC. The terminal voltage $\vec{V}_t$ is then processed by the PLL to extract the phase-locked angular frequency ω_p and phase angle θ_p, which establishes a PLL coordinate system. The current $\vec{I}$ is subsequently projected onto the PLL coordinate system to obtain the dq-axis currents (i_d^p, i_q^p). The deviations between the dq-axis currents (i_d^p, i_q^p) and corresponding reference (i_{dr}^p, i_{qr}^p) are fed into PI controllers to generate the dq-axis internal voltages (e_d^p, e_q^p). Finally, the dq-axis internal voltages (e_d^p, e_q^p), together with the PLL phase θ_p, form the internal-voltage reference $\vec{E}_r$, which is considered equal to the converter internal voltage $\vec{E}$ when the high-frequency pulse width modulation (PWM) process is neglected in this paper. Despite these simplifications, power converter units preserve the role of establishing the voltage, delivering active and reactive power [7].

B. Formation Mechanism of the grid-connected converter unit's Internal Voltage

According to the geometric illustration in Fig. 2(a), the instantaneous internal voltage E_{abc} reflects the projection of the internal-voltage rotating vector, which is determined by the frequency/amplitude of the internal voltage generated by the ACC, in the three-phase coordinate system, rather than being directly generated through a coordinate transformation from the dq-axis internal voltages (e_d^p, e_q^p) and the phase θ_p. In other words, the controlled variables of the ACC are essentially the radial length (internal-voltage amplitude A_e) and rotational angular frequency (internal-voltage angular frequency ω_e) of the rotating vector. The mathematical relationships are shown in (1) and (2).

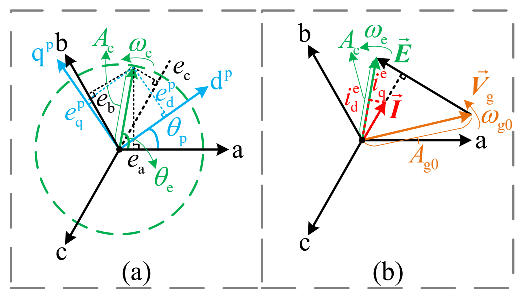

Fig. 2 Geometrical relationship among related electrical variables
(a) Forming mechanism of internal voltage (b) Forming mechanism of active/reactive current

$$\begin{cases} A_e = \sqrt{(e_d^p)^2 + (e_q^p)^2} \\ \omega_e = \omega_p + \dfrac{d}{dt}\arctan(\dfrac{e_q^p}{e_d^p}) \end{cases} \tag{1}$$

$$\begin{cases} \vec{E} = A_e e^{j(\int \omega_e dt + \theta_{e0})} \\ E_a = A_e \cos(\int \omega_e dt + \theta_{e0}) \\ E_b = A_e \cos(\int \omega_e dt + \theta_{e0} - \dfrac{2\pi}{3}) \\ E_c = A_e \cos(\int \omega_e dt + \theta_{e0} + \dfrac{2\pi}{3}) \end{cases} \tag{2}$$

Where θ_{e0} is the initial value of the internal-voltage rotating vector's phase.

C. Physical Interpretation of Active/Reactive Current

Under the combined stimulation of each unit's internal voltage, the current $\vec{I}$ at the grid-connected terminals of each unit responds according to the circuit topology constraints. For analytical convenience, the grid in Fig. 1 is modeled as a three-phase voltage source with constant amplitude and frequency, connected through the inductive transmission line, with its rotating vector defined in (3).

$$\vec{V}_g = A_{g0} e^{j(\int \omega_{g0} dt + \theta_{g0})} \tag{3}$$

979-8-3315-8138-1

Where A_{g0} is the constant amplitude of the voltage source, ω_{g0} is the constant angular velocity of the voltage source and is equal to the system synchronous angular velocity ω_0; θ_{g0} is the initial phase of the voltage-source rotating vector.

As illustrated in Fig. 2(b), the line current $\vec{I}$ is determined by the deviation between the internal voltage and the grid voltage through the inductance constraint relationship, which is given in (4).

$$\vec{I}=\frac{1}{L_{\text{eq}}}\int(\vec{E}-\vec{V}_{\text{g}})\text{d}t\triangleq A_{\text{i}}\,e^{\text{j}(\int\omega_{\text{i}}\,\text{d}t+\theta_{\text{i0}})} \tag{4}$$

Where $L_{eq} = L_f + L_g$, which is the total inductance between the grid voltage $\vec{V}_{\text{g}}$ and the unit's internal voltage $\vec{E}$. ω_i and A_i are the angular velocity and amplitude of the line current rotating vector, and θ_{i0} represents its initial phase.

As illustrated in Fig. 2(b), the line current $\vec{I}$ projected along the orientation of the internal voltage $\vec{E}$ yields the active current, representing the magnitude level of the instantaneous three-phase active power. The current $\vec{I}$ projected onto the orientation orthogonal to $\vec{E}$ yields the reactive current, representing the magnitude level of the instantaneous three-phase reactive power [8]. In the rotating coordinate system aligned with the internal voltage dq^{e}, the active and reactive currents aligned with the d-axis and q-axis correspond to i_{d}^{e} and i_{q}^{e}, with the corresponding vector projection relationship defined in (5).

$$\begin{aligned} i_{\text{d}}^{\text{e}}+\text{j}i_{\text{q}}^{\text{e}} &= \vec{I}e^{-\text{j}(\int\omega_{\text{e}}\text{d}t+\theta_{\text{e0}})}=A_{\text{i}}\,e^{\text{j}(\int\omega_{\text{i}}\,\text{d}t+\theta_{\text{i0}})-\text{j}(\int\omega_{\text{e}}\text{d}t+\theta_{\text{e0}})} \\ &= A_{\text{i}}\,e^{\text{j}(\int(\omega_{\text{i}}-\omega_{\text{e}})\text{d}t+\theta_{\text{i0}}-\theta_{\text{e0}})} \end{aligned} \tag{5}$$

D. Closed-loop operating principle between active/reactive current and internal-voltage amplitude/frequency in modern power systems

The role of the grid-connected converter units in power systems is to provide active and reactive power to meet users' demand and to cooperate with the network in maintaining the stability of the system's voltage and frequency [8]. To achieve this, the grid-connected converter units must regulate the internal-voltage frequency and amplitude based on the reactive/active current, thereby regulating the reactive and active power injected into the network. Meanwhile, the network must regulate the reactive/active current at each grid-connected terminal according to the frequency/amplitude of each grid-connected converter unit's internal voltage, thus ensuring a proper distribution of reactive/active power [9].

Although the grid-connected converter unit's internal-voltage amplitude/frequency is intuitively regulated by the combined stimulation of the line current $\vec{I}$ and the terminal voltage $\vec{V}_{\text{t}}$, in fact, $\vec{I}$ and $\vec{V}_{\text{t}}$ are both determined responses to the combined stimulation of each grid-connected converter unit's internal voltage $\vec{E}$. The relationship between the terminal voltage $\vec{V}_{\text{t}}$,line current $\vec{I}$, and the grid-connected unit's internal voltage $\vec{E}$ is shown in the blue shaded area in Fig. 3. The terminal voltage $\vec{V}_{\text{t}}$ is determined by the unit's internal voltage $\vec{E}$ and line current $\vec{I}$ through the filter inductance constraint relationship shown in (6). Therefore, the unit's internal-voltage amplitude/frequency is the response to the line current $\vec{I}$.

$$\vec{I}=\frac{1}{L_{\text{f}}}\int\left(\vec{E}-\vec{V}_{\text{t}}\right)\text{d}t \tag{6}$$

In summary, the unit essentially regulates its internal-voltage frequency/amplitude according to the active/reactive current. Accordingly, the network regulates the active/reactive current based on the internal-voltage amplitude/frequency. Therefore, the operation mechanism of converter-interfaced power systems can be depicted by a closed-loop regulation between the reactive/active current and the internal-voltage frequency/amplitude, as illustrated in Fig. 3.

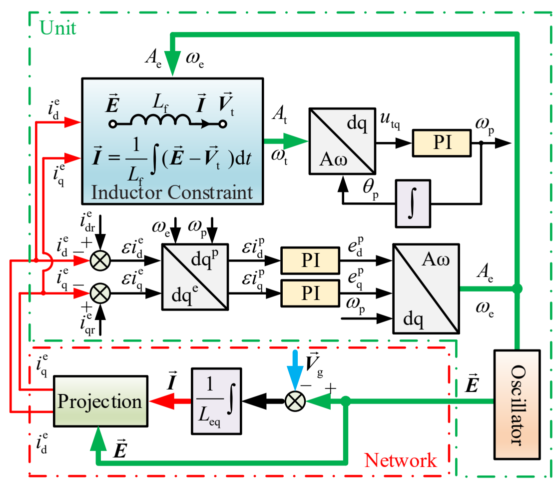

Fig. 3 Operation mechanism of converter-interfaced power systems

III. Damping Control Method Based on Amplitude and Frequency States

A. Energy-Exchange Mechanism of Converter-interfaced power system and State Interpretation of Internal-Voltage Amplitude/Frequency

The disturbance injects oscillatory power into the system, causing deviation between the reference and feedback active/reactive current, which leads to adjustments of the internal-voltage frequency/amplitude away from the steady-state operating point. The deviation between the reference and feedback reactive/active current directly reflects the imbalance of reactive/active power between the unit's input and output. To compensate for this imbalance, the unit must absorb or release the corresponding energy to the network, which changes its energy level and is manifested as a deviation of the internal-voltage amplitude/frequency from the steady-state operating point. This means that the dynamics of the internal-voltage frequency/amplitude reflect the time-cumulative effect of unbalanced active/reactive current. Therefore, the internal-voltage amplitude/frequency can be seen as state variables that characterize the energy storage level of the units.

979-8-3315-8138-1

The network, in turn, adjusts the active/reactive current at each terminal according to the internal-voltage frequency and amplitude of each unit, thereby supplying or absorbing the energy required or released by the unit. During this process, the amplitude/frequency, which represent the stored energy level, begin to oscillate. Through the constraint of (2), these oscillations regulate the internal voltage and, via the network constraints, couple to other electrical variables, eventually appearing as oscillations in the measured AC signals.

In summary, oscillations are essentially the observable manifestation of the exchange of reactive/active energy between the units and the networks, driven by the oscillatory power present in the system.

B. Structure of the Proposed Damping Control

The energy exchange between the units and the networks occurs widely between interacting energy-storing elements. In the mass-spring oscillating system shown in Fig. 4, when the spring is stretched and then released, the elastic potential energy represented by the deformation Δx and the kinetic energy represented by the mass velocity v convert into each other. Both the spring's deformation and the mass's velocity exhibit oscillatory behavior, indicating the system is oscillating.

To suppress system oscillations, the effective approach is to apply a damping force f_D, which is generated based on the state variable through an algebraic relationship, to the mass based on the mass's state variable v, to dissipate the unbalanced energy introduced by the disturbance, leading the system to return to its equilibrium state eventually. The example illustrates that the physical interpretation of damping lies in its role of dissipating unbalanced energy within the system.

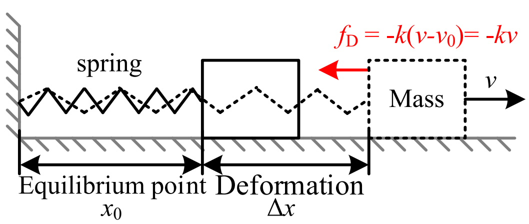

Fig. 4 Mass-spring oscillating system

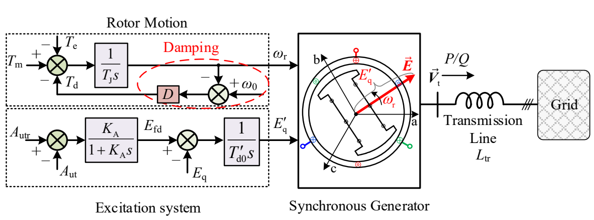

Fig. 5 Typical control structure of synchronous generator

The energy exchange process is analogous to that in the mass-spring oscillating system. The damping torque T_d shown in Fig. 5, which is generated based on the rotor speed ω_r, the state variable, through an algebraic relationship, represents the mechanical friction in the rotor motion. Power converter units are also driven by unbalanced power. Therefore, oscillation energy can be dissipated by introducing additional damping control, which changes the energy exchange characteristics between units and networks.

For the converter, active/reactive current imbalance serves as the stimulation, inducing dynamics in its energy level, reflected in deviations of the internal-voltage amplitude and frequency from their steady-state values. Based on the physical interpretation of damping, the proposed additional damping control, as illustrated in Fig. 6, generates the active/reactive damping current through an algebraic relationship that depends on amplitude and frequency states. Under the action of damping control, the energy exchange characteristics between units and networks are modulated, which can achieve the effect of dissipating oscillation energy, thereby suppressing system oscillations.

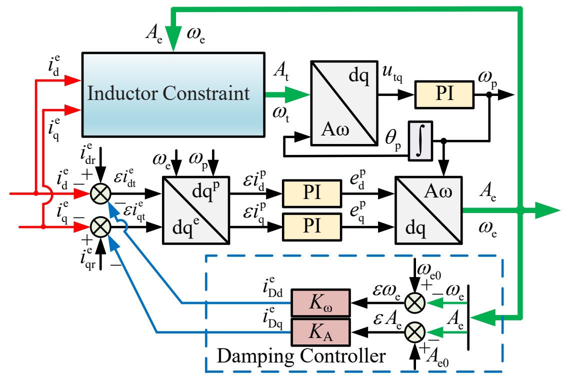

Fig. 6 Control mechanism of the grid-connected power converter unit with a damping controller

IV. SIMULATION AND VALIDATION

The effectiveness of the proposed method is validated through MATLAB/Simulink simulations conducted on a multi-converter power system. The corresponding system configuration and control structure are illustrated in Fig. 7. The detection of the internal-voltage amplitude and frequency can be realized through software-based algorithms as calculated in (1).

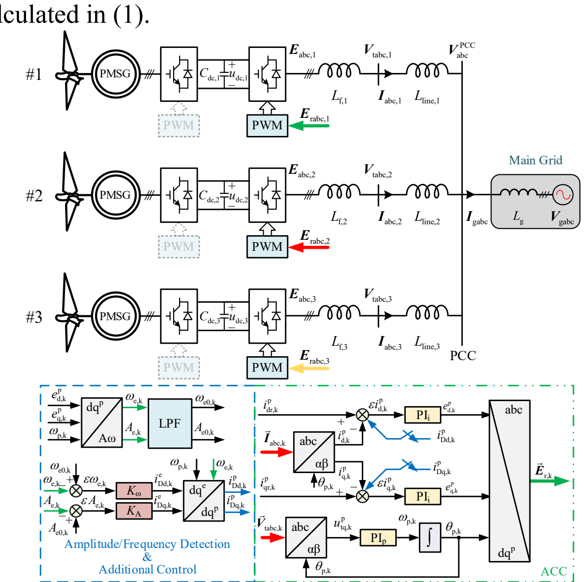

Fig. 7 System structure and Control structure used in simulation

A. *Case I: Verification under Sub-Synchronous Oscillation*

At Time = 0.2 s, a step disturbance is applied to the PLL angular velocity ω_p, causing a deviation of 0.5 rad/s from its operating point. This disturbance leads to an energy imbalance between the input and output of the converter, triggering energy exchange between the converter and the network and resulting in an 8.2 Hz sub-synchronous oscillation. After the damping controller is activated at Time = 3 s, the oscillatory power is dissipated by the active/reactive damping current, and the system gradually restores stability. The corresponding time-domain results of grid-connected unit #1 are illustrated in Fig. 8.

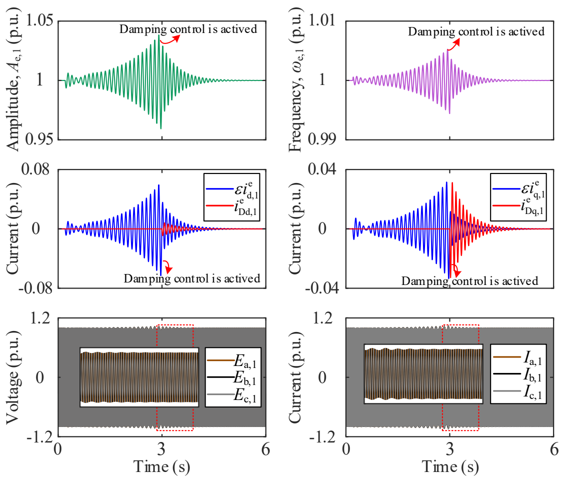

Fig. 8 Time-domain responses of grid-connected unit #1 under Case I

B. *Case II: Verification under Super-Synchronous Oscillation*

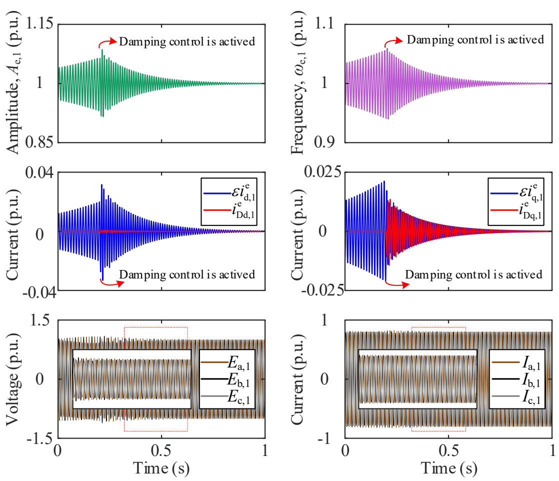

Fig. 9 Time-domain responses of grid-connected unit #1 under Case II

In Case II, the system is introduced to a similar disturbance in the PLL, leading to a 76 Hz super-synchronous oscillation. When the damping controller is activated at 0.2 s, the oscillation gradually mitigates, and the system returns to a stable operating state. The corresponding time-domain results of grid-connected unit #1 are illustrated in Fig. 9.

The results of Cases I and II indicate that the method can suppress emerging electromagnetic oscillations effectively by dissipating oscillatory power, demonstrating its effectiveness.

V. Conclusion

The study overcomes the limitation of existing methods that focus on superficial oscillation phenomena and lack the understanding of oscillation mechanisms. First, the operating mechanism of grid-connected power systems is uncovered, and the internal-voltage frequency and amplitude are seen as state variables that represent the energy level of the converter unit. Then, the oscillation mechanism is illustrated from the perspective of energy exchange. Finally, through elucidating the physical interpretation of damping, a damping method based on amplitude and frequency states is proposed. Simulation results verified that the method can effectively suppress oscillations by modulating energy exchange characteristics between units and networks.

References

[1] E. Leon and J. A. Solsona, "Sub-Synchronous Interaction Damping Control for DFIG Wind Turbines," *IEEE Transactions on Power Systems*, vol. 30, no. 1, pp. 419-428, Jan. 2015.

[2] H. Liu, X. Xie, J. He, T. Xu, C. Wang, et al., "Subsynchronous Interaction Between Direct-Drive PMSG Based Wind Farms and Weak AC Networks," *IEEE Transactions on Power Systems*, vol. 32, no. 6, pp. 4708-4720, Nov. 2017.

[3] Z. Xie, Y. Chen, W. Wu, X. Wang, and Z. Wang, "A global high-frequency oscillation suppression method for multi-inverter grid-connected system in weak grid," *Transactions of China Electrotechnical Society*, vol. 35, no. 4, pp. 885-895, Feb. 2020, (in Chinese).

[4] X. Tang, W. Zhang, and X. Zeng, "Resonance problem analysis and active suppression method for VSC-HVDC transmission system," *Proceedings of the CSEE*, vol 34, no. 30, pp. 5352-5359, Oct. 2014, (in Chinese).

[5] J. Dou, X. Tang, Y. Pan, J. Li, W. Qin, Y. Cai, et al, "Analysis and Suppression Method of Sub/Supersynchronous Oscillations for Grid-forming AC Grid-connected System with Virtual Impedance Control," in *Proc. 2025 30th International Conference on Automation and Computing*, pp. 1-6.

[6] X. Yuan and S. Wang, "Operating-Point Identification from Dimensions of Alternating Signal Based on Incremental Iterative Mapping Mechanism for Analyzing Dynamics of AC Systems," *CSEE Journal of Power and Energy Systems*, vol. 11, no. 1, pp. 163-172, Jan. 2025.

[7] X. Yuan, W. He, "Amplitude/Frequency as Prerequisites of Operation and Thus Classification of Stability Problems and Capability Opportunities for New Generations," *Journal of Power Supply*, vol. 19, no. 6, pp. 1-9, Nov. 2021, (in Chinese).

[8] H. Yang, X. Yuan, and W. He, "Active/reactive power generation mechanisms and representations in system dynamics with time-varying amplitude/frequency signals," *CSEE Journal of Power and Energy Systems*, Sept. 2024.

[9] R. Sun, H. Yang, W. He, and X. Yuan, "Electric Network Stimulation-Response Relationship and Its Characteristics Under Time-Varying Amplitude and Frequency," *IEEE Transactions on Industry Applications*, vol. 61, no. 3, pp. 4847-4861, June 2025.